AJNR

Evaluating Instantaneous Perfusion Responses of Parotid Glands to Gustatory Stimulation Using High-Temporal-Resolution Echo-Planar Diffusion-Weighted Imaging

T.-W. Chiu, Y.-J. Liu, H.-C. Chang, Y.-H. Lee, J.-C. Lee, K. Hsu, C.-W. Wang, J.-M. Yang, H.-H. Hsu and C.-J. Juan

AJNR Am J Neuroradiol 2016, 37 (10) 1909-1915
doi: https://doi.org/10.3174/ajnr.A4852
http://www.ajnr.org/content/37/10/1909

Evaluating Instantaneous Perfusion Responses of Parotid Glands to Gustatory Stimulation Using High-Temporal-Resolution Echo-Planar Diffusion-Weighted Imaging

T.-W. Chiu, Y.-J. Liu, H.-C. Chang, Y.-H. Lee, J.-C. Lee, K. Hsu, C.-W. Wang, J.-M. Yang, H.-H. Hsu, and C.-J. Juan

ABSTRACT

BACKGROUND AND PURPOSE: Parotid glands secrete and empty saliva into the oral cavity rapidly after gustatory stimulation. However, the role of the temporal resolution of DWI in investigating parotid gland function remains uncertain. Our aim was to design a high-temporal-resolution echo-planar DWI pulse sequence and to evaluate the instantaneous MR perfusion responses of the parotid glands to gustatory stimulation.

MATERIALS AND METHODS: This prospective study enrolled 21 healthy volunteers (M/F = 2:1; mean age, 45.2 ± 12.9 years). All participants underwent echo-planar DWI (total scan time, 304 seconds; temporal resolution, 4 s/scan) on a 1.5T MR imaging scanner. T2WI (b = 0 s/mm^2) and DWI (b = 200 s/mm^2) were qualitatively assessed. Signal intensity of the parotid glands on T2WI, DWI, and ADC was quantitatively analyzed. One-way ANOVA with post hoc group comparisons with Bonferroni correction was used for statistical analysis. $P < .05$ was statistically significant.

RESULTS: Almost perfect interobserver agreement was achieved ($\kappa \geq 0.656$). The parotid glands had magnetic susceptibility artifacts in 14.3% (3 of 21) of volunteers during swallowing on DWI but were free from perceptible artifacts at the baseline and at the end of scans on all images. Increased ADC and reduced signal intensity of the parotid glands on T2WI and DWI occurred immediately after oral administration of lemon juice. Maximal signal change of ADC (24.8% ± 10.8%) was significantly higher than that of T2WI (−10.1% ± 5.2%, $P < .001$). The recovery ratio of ADC (100.71% ± 42.34%) was also significantly higher than that of T2WI (22.36% ± 15.54%, $P < .001$).

CONCLUSIONS: Instantaneous parotid perfusion responses to gustatory stimulation can be quantified by ADC by using high-temporal-resolution echo-planar DWI.

ABBREVIATIONS: MSC = maximal signal change; RR = recovery ratio

Quantification of normal salivary gland function is of paramount clinical importance because it is the foundation of accurately evaluating disease-related salivary gland functional impairment. Salivary gland function can be estimated by several methods such as saliva collection,[1] laboratory measurement of the chemical and biochemical components,[2] scintigraphy,[3] single-photon emission CT,[4] and positron-emission tomography.[5] MR imaging is superior to saliva collection and laboratory and biologic studies by providing morphologic and functional information of the parotid glands simultaneously and specifically for individual salivary glands. On the other hand, MR imaging is also superior to scintigraphy, SPECT, and PET because of its high spatial resolution and radiation-free nature.

In recent decades, DWI has been increasingly applied to probe salivary gland function in addition to evaluating tumors,[6-11] connective tissue disorders,[12] Sjögren syndrome,[13,14] and postradiotherapy change[15-19] of the parotid glands. However, 2 mutually opposed trends of parotid apparent diffusion coefficient changes after gustatory stimulation have been observed in different study groups, even in healthy volunteers. While some researchers demonstrated an increase of parotid ADC after gustatory stimulation,[14,16,20-23] others showed a decrease of parotid ADC after this

Received November 16, 2015; accepted after revision April 3, 2016.

From the Departments of Radiology (T.-W.C., C.-W.W., H.-H.H., C.-J.J.) and Dentistry (K.H.), National Defense Medical Center, Taipei, Taiwan; Department of Medicine (T.-W.C.), Taipei Medical University, Taipei, Taiwan; Department of Automatic Control Engineering (Y.-J.L., Y.-H.L.), Feng Chia University, Taichung, Taiwan; Department of Diagnostic Radiology (H.-C.C.), The University of Hong Kong, Hong Kong; Department of Otolaryngology-Head and Neck Surgery (J.-C.L.), Tri-Service General Hospital, National Defense Medical Center, Taipei, Taiwan; Department of Biological Science and Technology (J.-C.L., J.-M.Y.), Institute of Bioinformatics and Systems Biology, National Chiao Tung University, Hsinchu, Taiwan; and Department of Radiology (C.-W.W., H.-H.H., C.-J.J.), Tri-Service General Hospital, Taipei, Taiwan.

Please address correspondence to Chun-Jung Juan, MD, PhD, Section of Radiology, School of Medicine, National Defense Medical Center, Section of Neuroradiology, Department of Radiology, Tri-Service General Hospital, 325, Section 2, Cheng-Kong Rd, Neihu, Taipei, Taiwan, Republic of China; e-mail: peterjuancj@yahoo.com.tw

http://dx.doi.org/10.3174/ajnr.A4852

stimulation.[15,24] Such discrepancy has been partially attributed to the different types and dosages of the stimulators.[16] Nevertheless, the discrepancy of diffusional responses to gustatory stimulation in the aforementioned DWI studies has raised concern for whether the normal salivary gland function has been evaluated appropriately with DWI.

The role of the temporal resolution of DWI, which might potentially influence researchers in interpreting parotid gland function, has not been documented to date, to our knowledge. Via parasympathetic innervation, salivary glands secrete and empty saliva into the oral cavity rapidly after gustatory stimulation. Current DWI studies might have limitations in catching the instantaneous responses of the parotid glands due to insufficient temporal resolution. We hypothesized that the parotid glands respond to the oral administration of lemon juice on the order of seconds. The aim of our study was to design a high-temporal-resolution echo-planar pulse sequence for DWI and to quantify the instantaneous MR perfusion responses of the parotid glands to gustatory stimulation.

MATERIALS AND METHODS

This prospective study was approved by the institutional review board at Tri-Service General Hospital. Written informed consent was obtained.

Subjects

This study initially enrolled 22 healthy volunteers who were free from tumor, inflammation, autoimmune disease, operations, and radiation therapy involving any parotid gland. One subject was excluded due to severe imaging distortion related to a fixed metallic dental brace. Finally, 21 healthy volunteers were enrolled, including 14 men and 7 women (mean age, 45.2 ± 12.9 years). Saliva production of each volunteer was quantified 1 hour before DWI by using the Saxon test.[1]

MR Imaging Protocol

All MR images were performed on a 1.5T whole-body scanner (Signa HDx; GE Healthcare, Milwaukee, Wisconsin) by using an 8NV head and neck array coil. Three-plane orthogonal gradient-echo images were acquired for anatomic localization. Single-shot echo-planar DWI (TR/TE/NEX, 2000/53.3 ms/1) with fat saturation was performed on axial planes with diffusion-probing gradients (b=0 and 200 s/mm^2) applied on each of 3 orthogonal directions alternatively. We intentionally chose a b-value of 200 s/mm^2 for 3 reasons: First, a b-value higher than 200 s/mm^2 has been shown to be perfusion-insensitive in ADC measurements.[25,26] Accordingly, choosing a b-value of 200 s/mm^2 allows better evaluation of perfusion-sensitive changes of the parotid glands than by using a b-value of 300 s/mm^2 or higher. Second, apparent bulk motion artifacts have been demonstrated in dynamic scans on DWI with a high b-value of 1000 s/mm^2 in the parotid glands.[27] On the contrary, DWI with a low b-value of 200 s/mm^2 has a higher signal-to-noise ratio[28] and is theoretically less susceptible to bulk motion artifacts than with higher b-values. Third, although it has been documented that b-values lower than 200 s/mm^2 are critical to obtain perfusion-sensitive information from DWI, there is no consensus on the magnitude of b-values that should be applied.[29] We chose a b-value of 200 s/mm^2 rather than 100 s/mm^2 to reduce potential contamination of signal loss from the faster flow of small arteries or veins. Other MR imaging parameters included an FOV of 240 × 240 mm, matrix size of 256 × 256, echo-train length of 76, bandwidth of 1953 Hz/pixel, and section thickness of 5 mm. Each DWI examination contained 152 excitations. Each excitation obtained 14 sections covering from the cerebellum to the submandibular glands. The total scan time was 5 minutes 4 seconds.

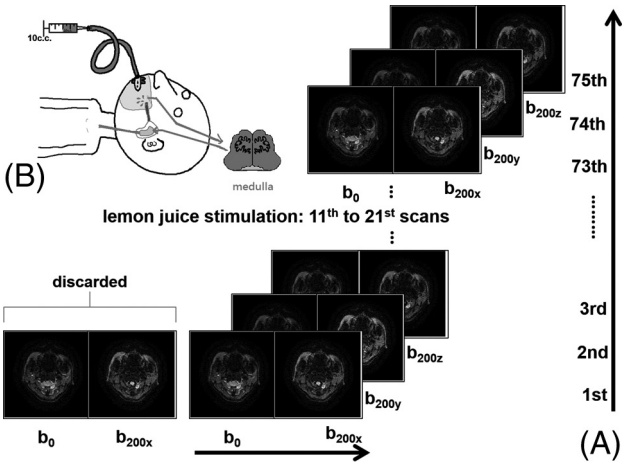

FIG 1. Demonstration of data acquisition and arrangement of DWI. *A*, The first 2 images were discarded. T2-weighted images (b_0) and diffusion-weighted images (b_{200}) were arranged alternatively for 75 dynamic scans. For DWI, diffusion gradients were applied along the x, y, and z axes periodically. *B*, Lemon juice was introduced into the oral cavity via a connecting tube at the 11th scan and swallowed at 21st scan. Figure 1*B* is courtesy of Cheng-Hsuan Juan.

MR Imaging Acquisition

T2WI (b = 0 s/mm^2) and DWI (b = 200 s/mm^2) were acquired alternatively. The first 2 excitations were discarded. The direction of the diffusion gradients was changed periodically in the order of the x, y, and z axes, allowing acquisition of a series of T2WI-DWI_x-T2WI-DWI_y-T2WI-DWI_z scans for the rest of the 150 excitations as illustrated in Fig 1*A*. Accordingly, 75 dynamic scans were used for analysis with each dynamic scan containing a T2WI and a DWI. The temporal resolution was 4 seconds per scan.

Gustatory Stimulation by Lemon Juice

As shown in Fig 1*B*, 10 mL of commercial lemon juice was administrated via a connecting tube into the oral cavity at the 11th dynamic scan. Each subject was instructed to swallow the lemon juice at the 21st scan. The duration of lemon juice stasis in the oral cavity was 40 seconds.

Qualitative Assessment of Imaging Quality

All MR imaging data were processed by software developed in-house (T.-W.C., Y.-H.L., and C.-J.J.) by using Matlab (MathWorks, Natick, Massachusetts). Magnetic susceptibility artifacts on T2WI and DWI were qualitatively and independently evaluated by 2 neuroradiologists (C.-J.J. and C.-W.W. with >10 and 3 years' experience in head and neck MR imaging interpretation, respectively) by using a 4-point grading score system (0, severe magnetic susceptibility artifacts: distortion and signal loss that

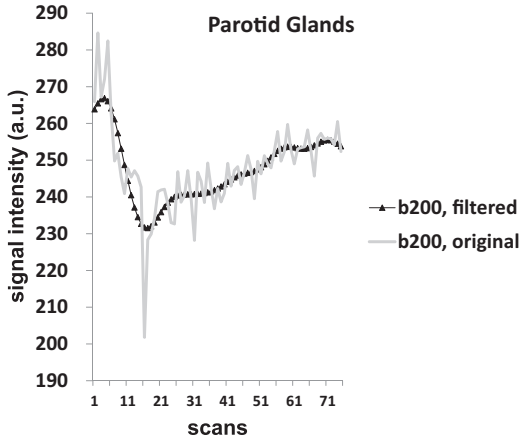

FIG 2. Signal intensity–time curves before and after fifth-order Butterworth low-pass filtering on DWI (b200). High-frequency noises (*gray peaks*) are apparently reduced, while the trend of time-series data in response to gustatory stimulation is preserved. a.u. indicates arbitrary unit.

involved the entire image; 1, moderate magnetic susceptibility artifacts: distortion and signal loss involving the parotid glands; 2, mild magnetic susceptibility artifacts: distortion and signal loss involving the oral cavity, nasal cavity, oropharynx, maxillary sinuses, or masticator spaces but sparing the parotid glands; and 3, no magnetic susceptibility artifacts). Qualitative analysis was performed on T2WI and DWI at baseline, during swallowing, and at the end of dynamic scans, respectively.

Imaging Processing and Quantitative Data Analysis

Quantitative analysis was performed on 3 contiguous sections covering the largest areas of the parotid glands, respectively. Polygonal ROIs were drawn within the bilateral parotid glands on the T2WIs, respectively, avoiding the partial volume effects from visible vessels and adjacent tissues. These ROIs were then automatically copied to the DWI for concurrent measurement of signal intensity. Time signal data of T2WI and DWI were treated by a fifth-order Butterworth low-pass filter with a cutoff frequency of 0.025Hz (Fig 2) to eliminate high-frequency noise that occurred during the dynamic scans.

ADC was calculated on the basis of the following equation:

$$1) \qquad ADC = \ln\frac{(S_{200} - S_0)}{-b},$$

where S_{200} and S_0 were signal intensities of images with b-values of 200 s/mm^2 and 0 s/mm^2, respectively. Signal intensity–time curves for T2WI, DWI, and ADC maps were plotted. In addition, signal intensity–time curves were further normalized according to equation 2:

$$2) \qquad SC_n = \frac{(SI_i - SI_0)}{SI_0},$$

where SC_n was the normalized signal change, SI_i was the signal intensity at the ith scan, and SI_0 was the baseline signal intensity averaged from the first 9 (first to ninth) scans. Salivary parameters, including maximal signal change (MSC), time to peak, and recovery ratio (RR), were further derived from the normalized signal change–time curves, respectively, to characterize the individual parotid responses to gustatory stimulation. MSC was defined as the maximal normalized signal change, TTP referred to the time interval from the start of dynamic scans to the time of MSC, and RR was calculated according to equation 3:

$$3) \qquad RR = \frac{(MSC - SC_{end})}{MSC},$$

where SC_{end} refers to the normalized signal change averaged from the last 9 (67th to 75th) scans.

Magnetic susceptibility artifact scores of T2WI and DWI

	At the Baseline		During Swallowing		At the End	
MSA Score	Rater 1	Rater 2	Rater 1	Rater 2	Rater 1	Rater 2
T2WI (b_0)						
0	0	0	0	0	0	0
1	0	1	0	1	0	1
2	20	19	20	19	20	19
3	1	1	1	1	1	1
DWI (b_{200})						
0	0	0	0	0	0	0
1	0	0	3	2	0	0
2	20	20	17	18	20	20
3	1	1	1	1	1	1

Note:—MSA indicates magnetic susceptibility artifacts.

Statistical Analysis

Statistical analysis was performed by using SPSS software (SPSS 20.0; IBM, Armonk, New York) and MedCalc for Windows (MedCalc Software, Mariakerke, Belgium). Interobserver reliability for imaging distortion was evaluated by linear-weighted κ statistics. The normality of baseline signal intensity and salivary parameters was analyzed by Kolmogorov-Smirnov tests. A paired Student *t* test was used for comparisons between the left and right parotid glands. Salivary parameters were analyzed by 1-way ANOVA; and post hoc group comparisons, with a Bonferroni correction. A P value $< .05$ was statistically significant.

RESULTS

The saliva collected within 2 minutes was 5.78 ± 2.61 g (mean ± standard deviation). Results of qualitative analysis of T2WI and DWI were summarized in the Table. Linear-weighted κ analysis revealed substantial agreement between the 2 raters with a κ value of 0.656 on all T2WIs and almost perfect agreement, with a κ value ranging from 0.842 (during swallowing) to 1 (at baseline and at the end of dynamic scans) on DWI. The parotid glands were free from perceptible artifacts at the baseline or at the end of scans on both T2WI and DWI (Fig 3). However, the parotid glands had magnetic susceptibility artifacts on DWI during swallowing in 14.3% (3 of 21) of volunteers who had metallic dental implants (Fig 4).

The left parotid glands did not differ from the right parotid glands in baseline signal intensity on either T2WI ($P = .148$) or DWI ($P = .227$). Therefore, data of both parotid glands of each subject were averaged to represent each individual in further analysis. Averaged signal intensity–time curves of the parotid glands on T2WI, DWI, and ADC were plotted in Fig 5. On both T2WI and DWI, the signal intensity decreased immediately after oral administration of lemon juice and kept declining during the gustatory stimulation. After swallowing, the signal intensity began to

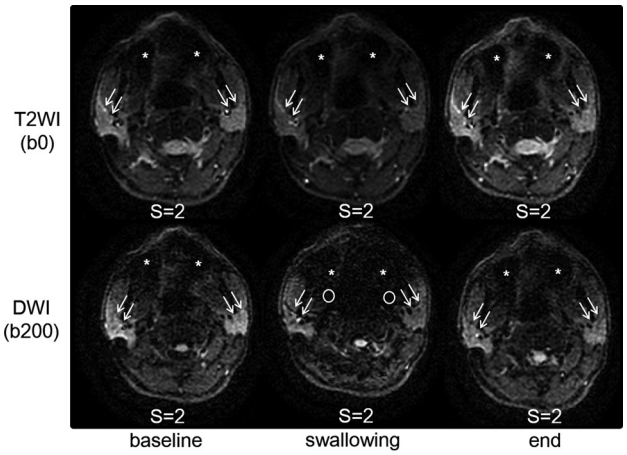

FIG 3. Magnetic susceptibility artifacts on T2WI and DWI. Mild distortion and signal loss involving the bilateral maxillary sinuses (*stars*) occur on all T2WI and DWI scans. During swallowing, the parotid glands are still free from artifacts, though more extensive artifacts involve the nasal cavity, oropharynx, and bilateral masticator spaces (*circles*). The anterior margins of the parotid glands are indicated by *arrows*. S indicates magnetic susceptibility artifact score.

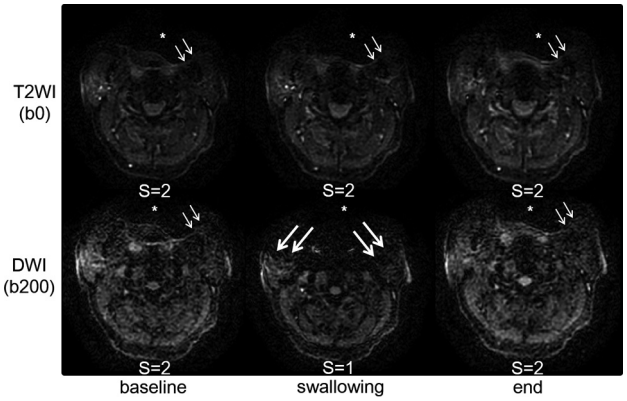

FIG 4. Magnetic susceptibility artifacts involving the bilateral masticator spaces and parotid glands (*long arrows*) are observed during swallowing on DWI in a volunteer with metallic dental implants. Artifacts involving the oral cavity (*stars*) and left masticator space (*short arrows*) are evident on all T2WI and DWI. S indicates magnetic susceptibility artifact score.

increase slowly on DWI but further dropped without perceptible recovery on T2WI (Fig 5*A*). On the contrary, the ADC increased abruptly during the lemon juice stimulation, reached the peak at swallowing, and then declined to the baseline level at the end of scans (Fig 5*B*).

Figure 6 demonstrates the normalized signal change–time curves of the parotid glands. The normalized signal change–time curves of the parotid glands on T2WI (Fig 6*A*), DWI (Fig 6*B*), and ADC (Fig 6*C*) revealed trends similar to signal intensity–time curves, respectively. One-way ANOVA showed significant differences in all salivary parameters, including MSC, TTP, and RR among T2WI, DWI, and ADC, respectively (all, $P \leq .001$). The results of post hoc analysis with Bonferroni correction of salivary parameters are described below. The MSC of ADC (24.8% ± 10.8%) was significantly higher than that of T2WI (−10.1% ± 5.2%; $P < .001$) and DWI (−14.2% ± 5.5%; $P < .001$). The MSC of T2WI did not differ from that of DWI ($P = .437$). TTP was significantly higher in T2WI (47.0 ± 17.3 scans) than in DWI (31.0 ± 16.4 scans; $P < .001$) and ADC (21.6 ± 11.1 scans; $P = .004$). There was no difference in TTP between DWI and ADC ($P = .132$). The RR of ADC (100.71% ± 42.34%) was significantly higher than in T2WI (22.36% ± 15.54%; $P < .001$) and DWI (42.3% ±21.7%; $P < .001$). There was no difference in RR between the T2WI and DWI ($P = .143$).

DISCUSSION

Temporal resolution is an important factor in analyzing immediate responses of the parotid glands to gustatory stimulation. Such immediate responses have not been emphasized in prior research,[14-16,20-24] in which DWI was performed without concurrent gustatory stimulation and the temporal resolution of DWI was rather low, ranging from 74 seconds per scan[21] to 162 seconds per scan.[16] Discrepant observations of parotid responses to the gustatory stimulation in prior research (ie, decreased ADC after gustatory stimulation in some studies[15,24] but increased ADC in others[14,16,20-23]) might be partly affected by the time gap between the gustatory stimulation and the poststimulation DWI and the low temporal resolution of DWI. Both factors limit DWI in detecting the maximal change of parotid ADC after gustatory stimulation.

In this prospective study, we successfully demonstrated the instantaneous responses of the parotid glands to gustatory stimulation by using echo-planar DWI at a high temporal resolution of 4 seconds. The overall signal intensity of the parotid glands on T2WI and DWI was altered at the start of stimulation, as was the parotid ADC. Our results support the hypothesis that the response of the parotid glands to gustatory stimulation occurs in seconds after oral intake of lemon juice.

On T2WI, the rapid reduction of signal intensity of the parotid glands might indirectly reflect an immediate reduction of saliva in the parotid glands after gustatory stimulation. Our result is consistent with the observations of quantitative salivary gland scintigraphic studies with a temporal resolution of 15 seconds per scan.[30] The immediate reduction of parotid radioactivity and accumulation of oral radioactivity following stimulation[30,31] supports saliva being emptied from the parotid glands immediately after the stimulation. After swallowing, the parotid glands showed persistent low signal intensity without recovery in averaged signal intensity–time curves and showed an RR of 22.36%, derived from individual signal intensity–time curves. Our results suggest that the refill of the water component of the parotid gland is a process longer than 3 minutes after removing the stimulator.

Because the signal intensity of vascular flow is attenuated rapidly under low b-values,[32] ADC calculated from low b-values (0 s/mm^2 and 200 s/mm^2) can be considered perfusion-sensitive in our study. Our study showed a maximal increase of 24.8% in the parotid ADC at 44.6 seconds (TTP = 21.6 scans) after the start of lemon juice stimulation. Such a rapid increase of parotid ADC implies an instantaneous increase of parotid perfusion after gustatory stimulation. The parotid response to gustatory stimulation has been recently investigated by arterial spin-labeling perfusion-weighted MR imaging,[33] showing a mean increase of 62% of parotid blood flow. However, arterial

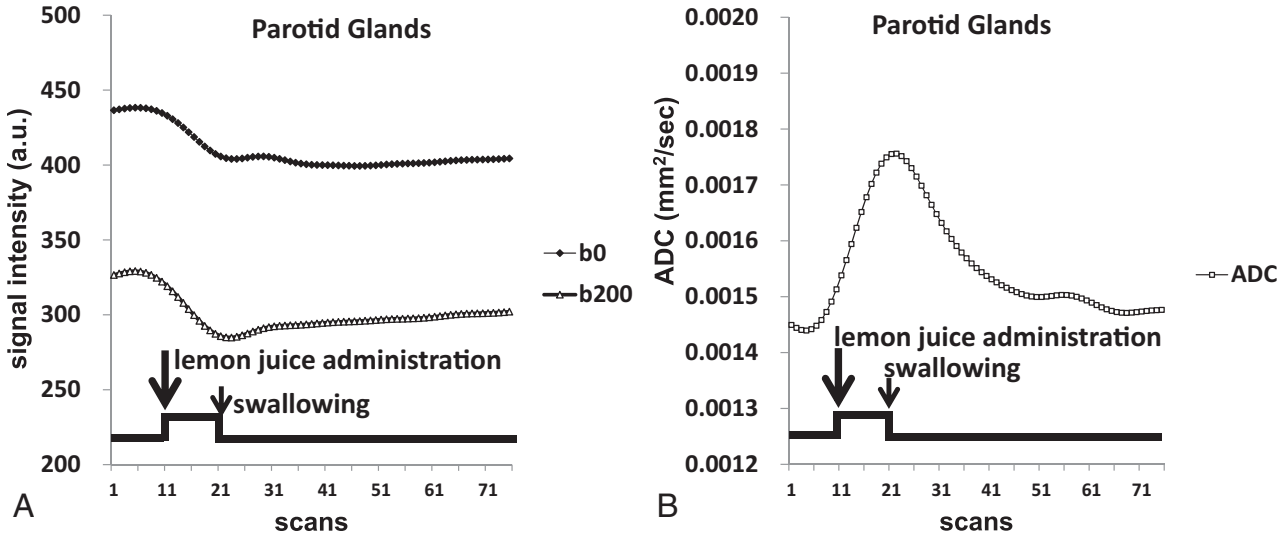

FIG 5. Averaged signal intensity–time curves of T2WI (b0) and DWI (b200) (*A*) and ADC time curves of the parotid glands (*B*). Lemon juice is administrated (*long arrow*) at the 11th scan and is swallowed (*short arrow*) at the 21st scan. a.u. indicates arbitrary unit.

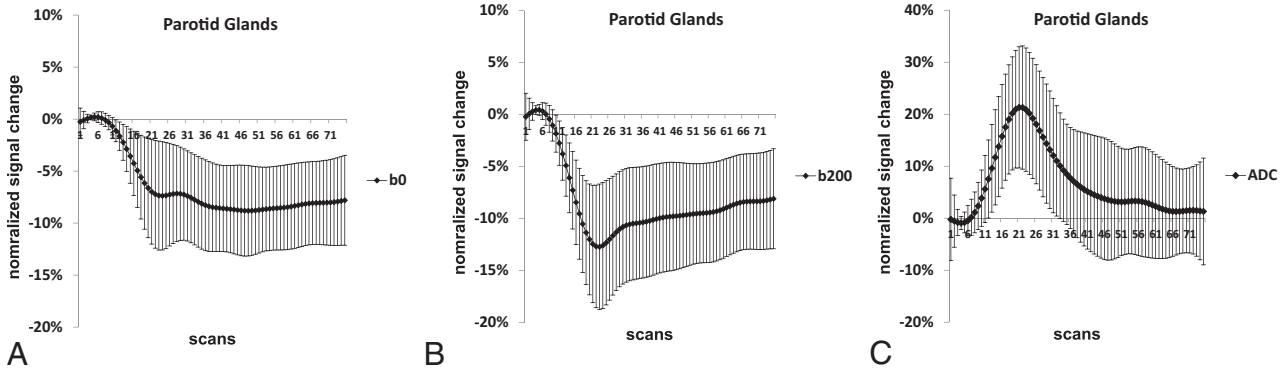

FIG 6. Normalized signal change–time curves (mean ± SD) of the parotid glands. During gustatory stimulation, the normalized signal change decreases rapidly on T2WI (*A*) and DWI (*B*), while it increases rapidly on ADC (*C*). After swallowing, the normalized signal change remains stagnant on T2WI, increases slowly on DWI, and reduces rapidly on ADC.

spin-labeling MR imaging is also limited in depicting the instantaneous response of the parotid glands due to its low temporal resolution of 160 seconds per scan.[33] Evaluation of parotid gland function by using blood oxygen level–dependent MR imaging showed an initial drop of signal intensity after gustatory stimulation by using ascorbic acid.[34] In addition to the aforementioned MR imaging techniques, dynamic contrast-enhanced MR imaging has also been applied to evaluate the perfusion change caused by salivary stimulation recently.[35] After swallowing, the parotid glands showed rapid reduction of ADC toward the baseline with an RR of 100% in our study. Our results reflect rapid reduction of parotid perfusion after swallowing lemon juice. The parotid ADC showed significantly higher RR than T2WI ($P < .001$). Our results suggest that the parotid perfusion has returned to the baseline level at the end of the dynamic scans, while the water refill of the parotid glands has not.

Our results also show apparent intersubject variations regarding all salivary parameters, especially after swallowing lemon juice. The intersubject variations might reflect the biologic diversity. If one takes TTP for example, possible reasons for the variations of TTP include residual lemon juice in the oral cavity, repeated swallowing, and other involuntary motions or background noises during dynamic scanning.

Our study has several potential limitations. First, there is a trade-off between temporal resolution and signal-to-noise ratio in our study. Therefore, we performed an analysis of imaging quality to examine the severity of magnetic susceptibility artifacts. Our results showed that the parotid glands were free from magnetic susceptibility artifacts at baseline and at the end of dynamic scans with substantial-to-almost perfect interobserver agreement. Second, the signal intensity of DWI might be influenced by bulk motion in our study. Therefore, we applied a low-pass filter to reduce the high-frequency signal fluctuations. Our results are consistent with the aforementioned quantitative salivary gland scintigraphic studies[30,31] regarding rapid emptying of saliva and arterial spin-labeling MR imaging studies[33] regarding increased blood flow after gustatory stimulation. Third, signal intensity on T2WI and DWI might be not only attributed to water molecules but also affected by fat molecules.[36,37] To verify the change of the water component in response to gustatory stimulation, another high-temporal-resolution echo-planar dual-echo MR imaging pulse sequence has been designed for direct measurement of the proton density of the parotid glands.

CONCLUSIONS

Instantaneous parotid perfusion responses to gustatory stimulation can be quantified by ADC by using high-temporal-resolution echo-planar DWI.

ACKNOWLEDGMENTS

The authors are grateful to Cheng-Hsuan Juan for contributing the comprehensive cartoon illustration of gustatory stimulation.

Disclosures: Y.-J. Liu—*UNRELATED: Grants/Grants Pending:* Received support in part from the Ministry of Science and Technology under Grant No. NSC 102-2221-E-035–003–MY.

REFERENCES

1. Kohler PF, Winter ME. **A quantitative test for xerostomia: the Saxon test, an oral equivalent of the Schirmer test.** *Arthritis Rheum* 1985; 28:1128–32 CrossRef Medline
2. Chiappin S, Antonelli G, Gatti R, et al. **Saliva specimen: a new laboratory tool for diagnostic and basic investigation.** *Clin Chim Acta* 2007;383:30–40 Medline
3. Arrago JP, Rain JD, Brocheriou C, et al. **Scintigraphy of the salivary glands in Sjögen's syndrome.** *J Clin Pathol* 1987;40:1463–67 CrossRef Medline
4. van Acker F, Flamen P, Lambin P, et al. **The utility of SPECT in determining the relationship between radiation dose and salivary gland dysfunction after radiotherapy.** *Nucl Med Commun* 2001;22: 225–31 CrossRef Medline
5. Buus S, Grau C, Munk OL, et al. **11C-methionine PET, a novel method for measuring regional salivary gland function after radiotherapy of head and neck cancer.** *Radiother Oncol* 2004;73:289–96 CrossRef Medline
6. Ikeda M, Motoori K, Hanazawa T, et al. **Warthin tumor of the parotid gland: diagnostic value of MR imaging with histopathologic correlation.** *AJNR Am J Neuroradiol* 2004;25:1256–62 Medline
7. Eida S, Sumi M, Sakihama N, et al. **Apparent diffusion coefficient mapping of salivary gland tumors: prediction of the benignancy and malignancy.** *AJNR Am J Neuroradiol* 2007;28:116–21 Medline
8. Yerli H, Agildere AM, Aydin E, et al. **Value of apparent diffusion coefficient calculation in the differential diagnosis of parotid gland tumors.** *Acta Radiol* 2007;48:980–87 CrossRef Medline
9. Yabuuchi H, Matsuo Y, Kamitani T, et al. **Parotid gland tumors: can addition of diffusion-weighted MR imaging to dynamic contrast-enhanced MR imaging improve diagnostic accuracy in characterization?** *Radiology* 2008;249:909–16 CrossRef Medline
10. Habermann CR, Arndt C, Graessner J, et al. **Diffusion-weighted echo-planar MR imaging of primary parotid gland tumors: is a prediction of different histologic subtypes possible?** *AJNR Am J Neuroradiol* 2009;30:591–96 CrossRef Medline
11. Celebi I, Mahmutoglu AS, Ucgul A, et al. **Quantitative diffusion-weighted magnetic resonance imaging in the evaluation of parotid gland masses: a study with histopathological correlation.** *Clin Imaging* 2013;37:232–38 CrossRef Medline
12. Patel RR, Carlos RC, Midia M, et al. **Apparent diffusion coefficient mapping of the normal parotid gland and parotid involvement in patients with systemic connective tissue disorders.** *AJNR Am J Neuroradiol* 2004;25:16–20 Medline
13. Sumi M, Takagi Y, Uetani M, et al. **Diffusion-weighted echoplanar MR imaging of the salivary glands.** *AJR Am J Roentgenol* 2002;178: 959–65 CrossRef Medline
14. Regier M, Ries T, Arndt C, et al. **Sjögren's syndrome of the parotid gland: value of diffusion-weighted echo-planar MRI for diagnosis at an early stage based on MR sialography grading in comparison with healthy volunteers.** *Rofo* 2009;181:242–48 CrossRef Medline
15. Dirix P, De Keyzer F, Vandecaveye V, et al. **Diffusion-weighted magnetic resonance imaging to evaluate major salivary gland function before and after radiotherapy.** *Int J Radiat Oncol Biol Phys* 2008;71: 1365–71 CrossRef Medline
16. Zhang Y, Ou D, Gu Y, et al. **Diffusion-weighted MR imaging of salivary glands with gustatory stimulation: comparison before and after radiotherapy.** *Acta Radiol* 2013;54:928–33 CrossRef Medline
17. Marzi S, Forina C, Marucci L, et al. **Early radiation-induced changes evaluated by intravoxel incoherent motion in the major salivary glands.** *J Magn Reson Imaging* 2015;41:974–82 CrossRef Medline
18. Juan CJ, Cheng CC, Chiu SC, et al. **Temporal evolution of parotid volume and parotid apparent diffusion coefficient in nasopharyngeal carcinoma patients treated by intensity-modulated radiotherapy investigated by magnetic resonance imaging: a pilot study.** *PLoS One* 2015;10:e0137073 CrossRef Medline
19. Studer G, Kirilova A, Jaffray D, et al. **Major salivary gland function: diffusion-weighted MRI (DWI) assessment before, during and after radiation therapy.** *International Journal of Radiation Oncology* 2005;63:S361 CrossRef
20. Habermann CR, Cramer MC, Graessner J, et al. **Functional imaging of parotid glands: diffusion-weighted echo-planar MRI before and after stimulation.** *Rofo* 2004;176:1385–89 CrossRef Medline
21. Habermann CR, Gossrau P, Kooijman H, et al. **Monitoring of gustatory stimulation of salivary glands by diffusion-weighted MR imaging: comparison of 1.5T and 3T.** *AJNR Am J Neuroradiol* 2007; 28:1547–51 CrossRef Medline
22. Ries T, Arndt C, Regier M, et al. **Value of apparent diffusion coefficient calculation before and after gustatory stimulation in the diagnosis of acute or chronic parotitis.** *Eur Radiol* 2008;18:2251–57 CrossRef Medline
23. Kato H, Kanematsu M, Toida M, et al. **Salivary gland function evaluated by diffusion-weighted MR imaging with gustatory stimulation: preliminary results.** *J Magn Reson Imaging* 2011;34: 904–09 CrossRef Medline
24. Thoeny HC, De Keyzer F, Claus FG, et al. **Gustatory stimulation changes the apparent diffusion coefficient of salivary glands: initial experience.** *Radiology* 2005;235:629–34 CrossRef Medline
25. Freiman M, Voss SD, Mulkern RV, et al. **In vivo assessment of optimal b-value range for perfusion-insensitive apparent diffusion coefficient imaging.** *Med Phys* 2012;39:4832–39 CrossRef Medline
26. Dikaios N, Punwani S, Hamy V, et al. **Noise estimation from averaged diffusion weighted images: can unbiased quantitative decay parameters assist cancer evaluation?** *Magn Reson Med* 2014;71: 2105–17 CrossRef Medline
27. Liu YJ, Lee YH, Chang HC, et al. **A potential risk of overestimating apparent diffusion coefficient in parotid glands.** *PLoS One* 2015;10: e0124118 CrossRef Medline
28. Lemke A, Stieltjes B, Schad LR, et al. **Toward an optimal distribution of b values for intravoxel incoherent motion imaging.** *Magn Reson Imaging* 2011;29:766–76 CrossRef Medline
29. Koh DM, Collins DJ, Orton MR. **Intravoxel incoherent motion in body diffusion-weighted MRI: reality and challenges.** *AJR Am J Roentgenol* 2011;196:1351–61 CrossRef Medline
30. Hermann GA, Vivino FB, Shnier D, et al. **Variability of quantitative scintigraphic salivary indices in normal subjects.** *J Nucl Med* 1998; 39:1260–63 Medline
31. Aung W, Murata Y, Ishida R, et al. **Study of quantitative oral radioactivity in salivary gland scintigraphy and determination of the clinical stage of Sjögren's syndrome.** *J Nucl Med* 2001;42:38–43 Medline
32. Koh DM. **Qualitative and quantitative analyses: image evaluation and interpretation.** In: Koh DM, Theony HC. *Diffusion-Weighted MR Imaging: Applications in the Body.* Berlin: Springer-Verlag; 2010:33–47
33. Schwenzer NF, Schraml C, Martirosian P, et al. **MR measurement of blood flow in the parotid gland without contrast medium: a functional study before and after gustatory stimulation.** *NMR Biomed* 2008;21:598–605 CrossRef Medline
34. Simon-Zoula SC, Boesch C, De Keyzer F, et al. **Functional imaging of the parotid glands using blood oxygenation level dependent**

(BOLD)-MRI at 1.5T and 3T. *J Magn Reson Imaging* 2008;27:43–48 CrossRef Medline

35. Clark HD, Moiseenko VV, Rackley TP, et al. **Development of a method for functional aspect identification in parotid using dynamic contrast-enhanced magnetic resonance imaging and concurrent stimulation.** *Acta Oncol* 2015;54:1686–90 CrossRef Medline
36. Juan CJ, Chang HC, Hsueh CJ, et al. **Salivary glands: echo-planar versus PROPELLER diffusion-weighted MR imaging for assessment of ADCs.** *Radiology* 2009;253:144–52 CrossRef Medline
37. Chang HC, Juan CJ, Chiu HC, et al. **Effects of gender, age, and body mass index on fat contents and apparent diffusion coefficients in healthy parotid glands: an MRI evaluation.** *Eur Radiol* 2014;24:2069–76 CrossRef Medline